



| | |
|------------------|--|
| Title | Performance of computed tomography-derived pulmonary vasculature metrics in the diagnosis and haemodynamic assessment of pulmonary arterial hypertension |
| Author(s) | Shimizu, Kaoruko; Tsujino, Ichizo; Sato, Takahiro; Sugimoto, Ayako; Nakaya, Toshitaka; Watanabe, Taku; Ohira, Hiroshi; Ito, Yoichi M.; Nishimura, Masaharu |
| Citation | European journal of radiology, 96, 31-38 https://doi.org/10.1016/j.ejrad.2017.09.010 |
| Issue Date | 2017-11 |
| Doc URL | http://hdl.handle.net/2115/71784 |
| Rights | © 2017. This manuscript version is made available under the CC-BY-NC-ND 4.0 license http://creativecommons.org/licenses/by-nc-nd/4.0/ |
| Rights(URL) | http://creativecommons.org/licenses/by-nc-nd/4.0/ |
| Type | article (author version) |
| File Information | EurJRadioI96_31.pdf |



[Instructions for use](#)

Title: Performance of computed tomography-derived pulmonary vasculature metrics in the diagnosis and haemodynamic assessment of pulmonary arterial hypertension

Abbreviations

AUC: area under the curve

BMI: body mass index

CI: cardiac index

%CSA_{<5}: cross-sectional area of small pulmonary vessels <5 mm² as a percentage of total lung area

CT: computed tomography

HU: Hounsfield units

ICC: intraclass correlation coefficient

ILD: interstitial lung disease

LOA: limit of agreement

PA/Ao: ratio of the diameter of the pulmonary artery to that of the aorta

PAH: pulmonary arterial hypertension

PAP: pulmonary arterial pressure

PH: pulmonary hypertension

PVD: ostial diameter of the right inferior pulmonary vein

PVR: pulmonary vascular resistance

RHC: right heart catheterization

ROC: receiver-operating characteristic curve

SSc: systemic sclerosis

Abstract

Background

Few studies have addressed the value of combining computed tomography-derived pulmonary vasculature metrics for the diagnosis and haemodynamic evaluation of pulmonary arterial hypertension (PAH).

Materials and methods

We measured three computed tomography parameters for the pulmonary artery, peripheral vessels, and pulmonary veins: the ratio of the diameter of the pulmonary artery to the aorta (PA/Ao), the cross-sectional area of small pulmonary vessels $<5 \text{ mm}^2$ as a percentage of total lung area (%CSA_{<5}), and the diameter of the right inferior pulmonary vein (PVD). The measured quantities were compared between patients with PAH (n = 45) and control subjects (n = 56), and their diagnostic performance and associations with PAH-related clinical indices, including right heart catheterization measurements, were examined.

Results

PA/Ao and %CSA_{<5} were significantly higher in patients with PAH than in controls. Receiver-operating characteristic curve analysis for ability to diagnose PAH showed a high area under the curve (AUC) for PA/Ao (0.95) and modest AUCs for %CSA_{<5} (0.75) and PVD (0.56). PA/Ao correlated positively with mean pulmonary arterial pressure and PVD correlated negatively with pulmonary vascular resistance. The %CSA_{<5} correlated negatively with mean pulmonary arterial pressure and pulmonary vascular resistance and positively with cardiac index. Notably, the PA/Ao and PVD values divided by %CSA_{<5} correlated better with right heart catheterization indices than the non-divided values.

Conclusion

PA/Ao, %CSA_{<5}, and PVD are useful non-invasive pulmonary vasculature metrics, both alone and in combination, for diagnosis and haemodynamic assessment of PAH.

Keywords: pulmonary arterial hypertension, pulmonary vasculature, pulmonary vein, CT, diagnosis, haemodynamic assessment

Introduction

Treatment for pulmonary arterial hypertension (PAH) has improved dramatically in recent years [1,2]. Early and accurate diagnosis of PAH has thus become critically important. Right heart catheterization (RHC) is mandatory for diagnosis of pulmonary hypertension (PH), and the current guidelines for PH recommend that RHC should be performed by well-trained physicians in high-volume PH centres [3].

Chest computed tomography (CT) is a less invasive and widely available imaging modality. To date, studies have reported the diagnostic value of plain CT-derived parameters, such as the diameter of the main pulmonary artery (PA) [4-6], the ratio of the diameter of the pulmonary artery to that of the aorta (PA/Ao) [7-10], and the segmental artery-to-bronchus ratio [11] in PH. In addition, recent studies have shown that the cross-sectional area of small pulmonary vessels $<5 \text{ mm}^2$ as a percentage of total lung area (%CSA_{<5}) reflects mean pulmonary arterial pressure (PAP) and is useful for diagnosis of PH in patients with emphysema or chronic obstructive pulmonary disease (COPD) [12-15]. However, the clinical relevance of %CSA_{<5} has not been examined in subjects without emphysema or COPD. The ostial diameter of the pulmonary vein (PVD) is another CT-derived metric that reflects PV pressure and flow [16] and is used in the field of interventional treatment for cardiac arrhythmias [17,18]. However, its clinical application in PH has not been investigated to date.

In the current study, we sought to examine the clinical value of three plain CT-derived indices of the pulmonary vasculature, i.e., PA/Ao, %CSA_{<5}, and PVD, in the diagnosis of PAH. Notably, these three indices reflect different parts of the pulmonary vasculature, and we hypothesised that combined use of these indices may be useful for the diagnosis and haemodynamic assessment of PAH.

Material and methods

Subjects

The protocol used in this retrospective study was approved by the ethics committee at Hokkaido University Hospital. All patients with PAH gave informed consent for their data to be included in the study. Our ethics committee gave permission for inclusion of the data for controls on the condition that online details of our study protocol are available in the public domain via the Hokkaido University Hospital website. The inclusion criteria for the PAH group were as

follows: (1) a resting mean PAP ≥ 25 mmHg and a pulmonary arterial wedge pressure ≤ 15 mmHg on RHC; (2) a diagnosis of PAH according to the 2015 guidelines for PH [3]; and (3) CT with/without contrast and RHC performed within 3 months of each other, during which time the patient's condition remained stable. The exclusion criteria were (1) any cardiovascular, respiratory, or other comorbidity that might affect the geometry of the thoracic aorta and/or pulmonary vasculature, (2) a forced expiratory volume in 1 second $< 60\%$ of predicted, and (3) a forced vital capacity $< 70\%$ of predicted [18]. We also studied controls matched for age and sex who fulfilled the following criteria: (1) no cardiac, respiratory, or other disease that might affect the geometry of the thoracic aorta and/or pulmonary vasculature, and (2) having chest CT data without contrast after December 2010 for screening or evaluation of lung nodules.

CT scanning

In this study, several types of scanners were used to capture the CT images, including Somatom Sensation 64 (Siemens, Munich, Germany), VCT (GE Healthcare, Little Chalfont, UK), Aquilion 64, Aquilion Prime, and Aquilion ONE ViSION Edition (Toshiba Medical Systems Corporation, Tochigi, Japan), and Brilliance iCT (Philips, Amsterdam, The Netherlands). The acquisition parameters and contrast media injection conditions were as follows: 100 kV, 0.5 s/rot, automatic exposure control (AEC), 450 mgI/kg, and injection 50 s for Somatom Sensation 64 and VCT; 120 kV, 0.5 s/rot, AEC, 480 mgI/kg, and injection 50 s for Aquilion 64; 120 kV, 0.5 s/rot, AEC, 450 mgI/kg, injection 50 s for Aquilion Prime; 120 kV, 0.4 s/rot, AEC, 480 mgI/kg, and injection 50 s for Aquilion ONE ViSION Edition; and 120 kV, 0.4 s/rot, AEC, 500 mgI/kg, and injection 50 s for Brilliance iCT.

CT measurements

Ratio of diameter of the pulmonary artery to that of the aorta

Measurements were acquired from axial CT images during inspiration. The interpreter measured the diameter of the main PA at the level of its bifurcation and that of the ascending aorta in its maximum dimension using the same images [19] (Figure 1A).

Cross-sectional area of small pulmonary vessels as a percentage of total lung area

We measured the %CSA₅ of three plain CT axial slices: 1 cm above the upper margin of the aortic arch (upper slice), 1 cm below the carina (middle slice), and 1 cm below the right inferior pulmonary vein (lower slice), using ImageJ software (National Institutes of Health, Bethesda,

MD, USA). We calculated the %CSA_{<5} using the method reported by Matsuoka et al [12], as outlined below.

We conducted the assessment of %CSA_{<5} using a bone reconstruction algorithm. The lung field consisted of all pixels between -500 and -1024 Hounsfield units (HU) on each CT slice. Then, segmented images were converted into binary images with a window level of -720 HU, allowing the identification of both pulmonary arteries and veins. A cross-sectional area of <5 mm² with a circularity within 0.9–1.0 for subsegmental levels of the pulmonary arteries and veins (CSA_{<5}) was measured in both lungs [20]. %CSA_{<5} is a ratio of CSA_{<5} to total lung area segmented by the threshold level between -500 and -1024 HU. In addition to the %CSA_{<5} of each slice, we calculated the average %CSA_{<5} of the three slices.

Diameter of the right inferior pulmonary vein

The diameter of the ostium of the right inferior pulmonary vein (PVD) was measured according to the method reported by Cronin et al [21] (Figure 1B). In brief, we chose a short-axis CT image that showed the ostium of the right PVD at its widest diameter and then measured the PVD.

Validity and reproducibility of the CT measurements

Fifteen patients with PAH were selected at random. One examiner ([name omitted for blinded review]) measured PA/Ao and PVD again to evaluate intraobserver variation, and another examiner ([name omitted for blinded review]) measured the two parameters to evaluate interobserver variation.

Interstitial lung shadows

The CT findings were determined according to the nomenclature recommendations of the Fleischner Society [22]. We defined ground-glass opacity, reticular opacity, honeycombing, traction bronchiectasis, and architectural distortion as interstitial lung shadows [6]. The presence of interstitial change in the lungs was assessed by radiologists and a pulmonologist who were unaware of the clinical data, including the results of RHC and the treatment regimens used for PAH.

Statistical analysis

The patients' demographic characteristics, the results of their pulmonary function tests, and

analysis of CT imaging data are shown as the mean \pm standard deviation. The Wilcoxon' test or *t*-test was used to compare CT parameters between the PAH and control groups as appropriate.

The sensitivity, specificity, positive predictive value (PPV), and negative predictive value (NPV) of PA/Ao, %CSA_{<5}, and PVD for the diagnosis of PAH was estimated by receiver-operating characteristic (ROC) curve analysis. For each CT index, the cut-off level was defined as 2 standard deviations above the mean in the control group.

Pearson's correlation coefficient was used to test for correlations between the CT parameters and the results of RHC. We also sought correlations of the ratios of the PA/Ao divided by %CSA_{<5} (of the upper, middle, or lower slice) and the PVD divided by %CSA_{<5} (of the upper, middle, or lower slice) with the RHC data, on the assumption that such ratios may better predict RHC data because each CT index reflects a different site in the pulmonary vasculature. Multivariate regression analysis was performed to examine if the three CT parameters (i.e., PA/Ao, %CSA_{<5}, and PVD) had correlations with RHC parameters independently of each other. Multivariate regression was also used to determine whether these three CT parameters had correlations with RHC parameters independently of two confounding factors: systemic sclerosis (SSc) [23] and the presence of interstitial lung shadow(s) .

Regarding the validity and reproducibility of the CT measurements, we calculated the limits of agreement (LOAs), as determined using the Bland-Altman method, and the intraclass correlation coefficients (ICCs) for interobserver and intraobserver variation.

All statistical computations were performed using JMP version 12 software (SAS Institute Inc, Cary, NC, USA). A p-value <0.05 was considered to be statistically significant.

Results

We reviewed our clinical records for patients with PAH who underwent CT between March 2003 and July 2015 and identified 45 patients who met the study eligibility criteria (Figure 2).

We measured the diameters of the PA, Ao, and PVD, and calculated PA/Ao in these subjects (PA/Ao group, n = 45). The %CSA_{<5} was calculated in 20 of the subjects (%CSA_{<5} group) because of use of contrast medium or inadequate acquisition of CT parameters in the remaining 25 subjects. We also recruited 56 controls matched for age and sex for comparative purposes.

The demographics of the patients with PAH and the controls are summarised in Table 1. There was no significant difference in any parameter between the control group and the two PAH groups. Table 2 shows the PH-related data for the PA/Ao group and the %CSA_{<5} group.

PA/Ao and %CSA_{<5} were significantly higher in the PAH group than in the control group, with no difference in PVD between the groups (Figure 3). The %CSA_{<5} values for the middle, and lower slices were significantly higher in patients with PAH than in controls, whereas that for the upper slice was not (Table 3).

As shown in Figure 4, the AUC for ability to diagnose PAH was high for PA/Ao (0.955) and modest for %CSA_{<5} (0.748) and PVD (0.560). The AUCs for %CSA_{<5} were 0.634, 0.752, and 0.733 for the upper, middle, and lower slices, respectively. The sensitivity, specificity, PPV, and NPV of the CT indices for diagnosis of PH are summarised in Table 4. The cut-off values applied were 0.99 for PA/Ao, 14.89 for PVD, and 0.478 for %CSA_{<5}. The diagnostic performance of PA/Ao was also examined using a cut-off level of 1.00. The results indicated that PA/Ao had better diagnostic accuracy than %CSA_{<5} or PVD at cut-off values of 0.99 and 1.00.

PA/Ao correlated positively with mean PAP (Figure 5A), PVD correlated negatively with pulmonary vascular resistance (PVR) (Figure 5B), and %CSA_{<5} correlated negatively with mean PAP and PVR and positively with the cardiac index (CI) (Figure 5C). The %CSA_{<5} of the upper slice showed stronger correlations with mean PAP, CI, and PVR than the %CSA_{<5} of the middle and lower slices (Table 5).

Multivariate analysis revealed that %CSA_{<5} independently correlated with mean PAP, CI, and PVR ($t = -2.79$, $p = 0.014$ for mean PAP; $t = 4.48$, $p = 0.0004$ for CI; $t = -2.42$, $p = 0.03$ for PVR), whereas PA/Ao and PVD did not have significant and independent correlations with any RHC index. Multivariate regression analysis also showed similar results regarding the correlations between CT indices and the RHC data (Figure 5A–5C), independent of the presence of SSc or interstitial lung shadows (Table 6).

The PAH and control groups did not have significantly different values of PA/Ao divided by mean %CSA_{<5} ($p = 0.81$) or PA/Ao divided by %CSA_{<5} of the upper ($p = 0.17$), middle ($p = 0.51$), or lower lung slices ($p = 0.89$). As compared with controls, patients with PAH had significantly lower values of PVD divided by mean, middle-slice, and lower-slice %CSA_{<5} ($p = 0.01$, $p = 0.004$, and $p = 0.03$, respectively). However, PVD divided by upper-slice %CSA_{<5} did not differ significantly between the two groups ($p = 0.24$). Table 7 shows correlations between RHC data and the ratios of PA/Ao and PVD to %CSA_{<5} for the three slice levels. PA/Ao divided

by the %CSA_{<5} of the upper slice was significantly correlated with mean PAP, PVR, and CI (Figure 6A) and had higher correlation coefficients than those for PA/Ao (Figure 5A) and the %CSA_{<5} of the upper slice (Figure 5B) alone. Similarly, PVD divided by %CSA_{<5} of the upper slice (Figure 6B) correlated better with RHC parameters than the PVD (Figure 5B) or %CSA_{<5} of the upper slice (Figure 5C).

Validity and reproducibility of the CT measurements

Examining measures of intraobserver variation showed that the LOA (mean difference \pm 2 standard deviations) was 0.0003 ± 0.04 and the ICC was 0.93 for PA/Ao, while the LOA was 0.84 ± 0.5 and the ICC was 0.73 for PVD. Regarding interobserver variation, the LOA was 0.03 ± 0.06 and the ICC was 0.86 for PA/Ao, while the LOA was 0.67 ± 0.5 and the ICC was 0.76 for PVD.

Discussion

The current retrospective observational study demonstrated an increased PA/Ao in patients with PAH and a high AUC of PA/Ao for the diagnosis of PAH. Further, PA/Ao, %CSA_{<5}, and PVD showed significant correlations with mean PAP, CI, and PVR. Notably, the PA/Ao and PVD values divided by %CSA_{<5} correlated better with RHC indices than the non-divided values. These results suggest that combined evaluation of PA/Ao, %CSA_{<5}, and PVD is a useful non-invasive measure for diagnosis and haemodynamic assessment of PAH.

Studies have shown that PA/Ao is increased in PH [7-10,19]. The elevated PA/Ao observed in the present study compared well with values in previous publications [5,6,8,11,24]. Further, the high AUC of the PA/Ao for diagnosis of PAH and its significant correlation with mean PAP were also consistent with the previous studies. In our study population, PA/Ao was confirmed to be a simple plain CT-derived index that offers high sensitivity for the diagnosis of PH and reflects the degree of elevation of PAP.

Importantly, the previous studies of %CSA_{<5} did not examine any control subjects [12,15]. In the present study, we included both control and PAH groups, and the obtained results notably suggest that %CSA_{<5} might be useful as a screening tool for the diagnosis of PH. The greater %CSA_{<5} values that we observed in patients with PAH may be explained by elevated pressure within the pulmonary arteries, which likely expanded these arteries, leading to higher %CSA_{<5} values. Other possible explanations for the greater %CSA_{<5} values in patients with PAH include thickening of the intima/media/adventitia of the pulmonary arteries [25,26], as well as reopening of the peripheral pulmonary arteries [27,28], which is known to occur in

the pulmonary peripheral vasculature during exercise and in left heart failure [29].

In the present study, %CSA_{<5} had a significant, negative correlation with mean PAP, similar to the previous study by Matsuoka et al [12]. We speculate that the negative correlation may be an effect of reduced CO in advanced PH cases. In such cases, CO can be low even when PAP remains high [30, 31], and low CO causes reduced blood flow in the pulmonary veins, leading to reduced sizes of the pulmonary veins and resultant decreases in %CSA_{<5}. This speculation is supported by the significant, negative association between CI and %CSA_{<5} shown in Figure 5. Additionally, as was speculated by Matsuoka et al, reduced distensibility of the vascular walls in advanced cases might underlie the negative correlation between the two indices. However, these speculations were not verified in the present study because we neither were able to distinguish arteries from veins in the analysis of CT images, nor directly measured the distensibility of the vessels. Thus, the mechanisms behind the negative association between mean PAP and %CSA_{<5} remain to be elucidated.

Multivariate analyses in the present study showed %CSA_{<5} independently correlated with mean PAP, CI, and PVR, but PA/Ao and PVD did not demonstrate such a correlation. These results indicate that %CSA_{<5} reflects the pathophysiology of PAH better than do PA/Ao and PVD. Interestingly, however, the diagnostic performance of %CSA_{<5} was poorer than that of PA/Ao, as shown in Figure 4. This discrepancy may be attributed to a non-linear relationship between %CSA_{<5} and mean PAP in a combined cohort of control and PAH subjects, which is in contrast to the positive linear association between PA/Ao and mean PAP. In fact, %CSA_{<5} can be increased in early stage PAH but, conversely, reduced in advanced PAH patients with low CI, which can decrease the sensitivity of %CSA_{<5} for the diagnosis of PH.

It is noteworthy that the %CSA_{<5} value of the upper slice correlated strongly with the mean PAP, PVR, and CI, while the %CSA_{<5} values of the middle and lower slices did not. This variation in results between the three slice levels may be attributable to the methodology used to calculate %CSA_{<5} in this study. We analysed round opacities with a circularity between 0.9 and 1.0. This may have resulted in better detection of morphological changes in the vessels of the upper lung, where vessels run more perpendicularly to the slice than they do for the other slice levels. Further, greater susceptibility to reopening [30,31] or more advanced vasculopathy in the upper lungs might have caused the stronger relationship between %CSA_{<5} in the upper lung and the RHC results.

We found that two indices, i.e., PA/Ao/(%CSA_{<5} of the upper slice) and PVD/(%CSA_{<5} of the upper slice) correlated with RHC indices more strongly than PA/Ao, PVD, or %CSA_{<5}. The stronger correlations between the ratios of the CT indices and the RHC data over the individual

CT indices can be explained as follows. As PAP rises, the PA/Ao is likely to increase because of the increased outward pressure on the wall of the PA. In contrast, the %CSA_{<5} may decrease in patients with advanced PAH as discussed above. This may explain why PA/Ao divided by %CSA_{<5} better predicted RHC data than PA/Ao or %CSA_{<5} alone. Alternatively, %CSA_{<5} and PVD are vascular parameters that are located upstream and downstream of the diseased arterioles, respectively, which may lead to altered associations with RHC parameters of PVD/(%CSA_{<5} of the upper slice) as compared with PVD or %CSA_{<5} alone.

SSc is a systemic disorder characterised by progressive fibrosis in various organs [32,33]. The pulmonary vessels and myocardium can be involved in SSc, and this may have been a potential source of bias in this study. Further, the presence of interstitial lung disease (ILD) may hamper the diagnostic value of %CSA_{<5} in particular because small opacities attributable to ILD cannot be distinguished from those of the pulmonary vasculature. However, multivariate analysis in the present study showed that %CSA_{<5} correlated with RHC parameters independent of the presence of SSc or ILD, suggesting an independent relevance of CT metrics for the diagnosis and haemodynamic assessment of PH. However, in this study, there were only four patients with SSc and the degree of ILD was mild. Therefore, the potentially confounding effects of SSc and ILD need to be investigated further.

There are several limitations to this study. First is its retrospective design and small patient population. The %CSA_{<5} was assessed in only 20 patients, so the study may not have been adequately powered to identify statistically significant differences and/or associations between the study parameters. Second, we adopted automatic exposure control, which could have substantially affected the measurement of %CSA_{<5}. Especially, the required radiation dose varies depending on body mass index (BMI). For instance, an effective dose is about 3500 mAs for a BMI of 18, while it is more than 6500 mAs for a BMI of 35 [34]. The BMIs of the PAH and the control groups were similar in our study (mean \pm standard deviation: PAH: 23.4 ± 4.3 , controls: 22.8 ± 4.0 , $p > 0.05$). Nonetheless, we could not exclude the possibility that applying the automatic exposure control might have affected %CSA_{<5}, thereby confounding the associations between %CSA_{<5} and the RHC data. Third, in the present study, we did not include the echocardiography-derived indices in the analyses, even though echocardiography is a widely used non-invasive modality for the assessment of morphology/function of the right heart [35]. Echocardiography also enables the evaluation of the pulmonary haemodynamics using Doppler methods. However, chest CT is commonly used, particularly among pulmonologists, and its image quality is consistently favourable, independent of the body habitus and the shape and size of the right heart. We thus believe that applying CT to assess PH may have an additional or complementary role, even in clinical settings where echocardiography is available. Fourth, the

aetiology of PAH was variable and likely to affect the vascular and cardiac macro/microstructure. Thus, this variation could have affected the study results. Fifth, CT and RHC were performed within 3 months of each other but not simultaneously. However, we used CT and RHC data from patients who were clinically stable with no remarkable changes in the results of laboratory or radiological examinations during the study period. Sixth, we included patients regardless of use of medication and cannot exclude the possibility that medications approved for the treatment of PAH affected the morphology of the pulmonary vasculature and/or the heart, subsequently affecting associations between the CT and RHC indices. Finally, given the retrospective nature of the study, it was inevitable that several types of CT scanner were used to acquire the study measurements.

In conclusion, we found the PA/Ao to be a simple CT-derived index that was useful for diagnosis of PAH. In this study, PVD and %CSA_{<5} did not have high accuracy for diagnosis of PAH, but were associated with the CI and/or PVR. Further, the ratios of PA/Ao and PVD to %CSA_{<5} were strongly correlated with measures of pulmonary haemodynamics. These findings suggest that non-invasive CT indices are clinically relevant in the diagnosis and haemodynamic assessment of PAH.

Funding source

This research did not receive any specific grant from funding agencies in the public, commercial, or not-for-profit sectors.

Conflicts of interest

None.

References

- [1] T. Pulido, I. Adzerikho, R.N. Channick, M. Delcroix, N. Galiè, H.A. Ghofrani, P. Jansa, Z.C. Jing, F.O. Le Brun, S. Mehta, et al; SERAPHIN Investigators, Macitentan and morbidity and mortality in pulmonary arterial hypertension, *N. Engl. J. Med.* 369 (2013) 809–818.
- [2] N. Galiè, J.A. Barberà, A.E. Frost, H.A. Ghofrani, M.M. Hoeper, V.V. McLaughlin, A.J. Peacock, G. Simonneau, J.L. Vachiery, E. Grünig, et al; AMBITION Investigators, Initial use of ambrisentan plus tadalafil in pulmonary arterial hypertension, *N. Engl. J. Med.* 373 (2015) 834–844.
- [3] N. Galiè, M. Humbert, J.L. Vachiery, S. Gibbs, I. Lang, A. Torbicki, G. Simonneau, A.

Peacock, A. Vonk Noordegraaf, M. Beghetti, et al, 2015 ESC/ERS Guidelines for the diagnosis and treatment of pulmonary hypertension: The Joint Task Force for the Diagnosis and Treatment of Pulmonary Hypertension of the European Society of Cardiology (ESC) and the European Respiratory Society (ERS): Endorsed by: Association for European Paediatric and Congenital Cardiology (AEPC), International Society for Heart and Lung Transplantation (ISHLT), *Eur. Respir. J.* 46 (2015) 903–975.

[4] K. Kuriyama, G. Gamsu, R.G. Stern, C.E. Cann, R.J. Herfkens, B.H. Brundage, CT-determined pulmonary artery diameters in predicting pulmonary hypertension, *Invest. Radiol.* 19 (1984) 16–22.

[5] C.S. Ng, A.U. Wells, S.P. Padley, A CT sign of chronic pulmonary arterial hypertension: the ratio of main pulmonary artery to aortic diameter, *J. Thorac. Imaging.* 14 (1999) 270–278.

[6] E.H. Alhamad, A.A. Al-Boukai, F.A. Al-Kassimi, H.F. Alfaleh, M.Q. Alshamiri, A.H. Alzeer, H.A. Al-Otair, G.F. Ibrahim, S.A. Shaik, Prediction of pulmonary hypertension in patients with or without interstitial lung disease: reliability of CT findings, *Radiology.* 260 (2011) 875–883.

[7] C. Dornia, T.J. Lange, G. Behrens, J. Stiefel, R. Müller-Wille, F. Poschenrieder, M. Pfeifer, M. Leitzmann, D. Manos, J.L. Babar, et al, Multidetector computed tomography for detection and characterization of pulmonary hypertension in consideration of WHO classification, *J. Comput. Assist. Tomogr.* 36 (2012) 175–180.

[8] A. Mahammedi, A. Oshmyansky, P.M. Hassoun, D.R. Thiemann, S.S. Siegelman, Pulmonary artery measurements in pulmonary hypertension: the role of computed tomography, *J. Thorac. Imaging.* 28 (2013) 96–103.

[9] S. Rajaram, A.J. Swift, D. Capener, C.A. Elliot, R. Condliffe, C. Davies, C. Hill, J. Hurdman, R. Kidling, M. Akil, et al, Comparison of the diagnostic utility of cardiac magnetic resonance imaging, computed tomography, and echocardiography in assessment of suspected pulmonary arterial hypertension in patients with connective tissue disease, *J. Rheumatol.* 39 (2012) 1265–1274.

[10] N. Corson, S.G. Armato 3rd, L.E. Labby, C. Straus, A. Starkey, M. Gomberg-Maitland, CT-based pulmonary artery measurements for the assessment of pulmonary hypertension, *Acad. Radiol.* 21 (2014) 523–530.

[11] D. Pérez-Enguix, P. Morales, J.M. Tomás, F. Vera, R.M. Lloret, Computed tomographic screening of pulmonary arterial hypertension in candidates for lung transplantation, *Transplant. Proc.* 39 (2007) 2405–2408.

[12] S. Matsuoka, G.R. Washko, T. Yamashiro, R.S. Estepar, A. Diaz, E.K. Silverman, E. Hoffman, H.E. Fessler, G.J. Criner, N. Marchetti, et al, National Emphysema Treatment Trial Research Group. Pulmonary hypertension and computed tomography measurement of small pulmonary vessels in severe emphysema, *Am. J. Respir. Crit. Care Med.* 181 (2010) 218–225.

- [13] S. Matsuoka, G.R. Washko, M.T. Dransfield, T. Yamashiro, R. San Jose Estepar, A. Diaz, E.K. Silverman, S. Patz, H. Hatabu, Quantitative CT measurement of cross-sectional area of small pulmonary vessel in COPD: correlations with emphysema and airflow limitation, *Acad. Radiol.* 17 (2010) 93–99.
- [14] S. Matsuoka, T. Yamashiro, S. Matsushita, A. Kotoku, A. Fujikawa, K. Yagihashi, H. Tomita, S. Sakamoto, Y. Saito, S. Saruya, et al, Usefulness of coronal reconstruction CT images for quantitative evaluation of the cross-sectional area of small pulmonary vessels, *Acad. Radiol.* 21 (2014) 1411–1415.
- [15] F. Coste, G. Dournes, C. Dromer, E. Blanchard, V. Freund-Michel, P.O. Girodet, M. Montaudon, F. Baldacci, F. Picard, R. Marthan, et al, CT evaluation of small pulmonary vessels area in patients with COPD with severe pulmonary hypertension, *Thorax.* 71 (2016) 830–837.
- [16] Kittleson MD, editor. Chapter 4: Radiography of the cardiovascular system. Veterinary Information Network: Davis, CA, USA: 2015.
- [17] M.R. Jongbloed, M.S. Dirksen, J.J. Bax, E. Boersma, K. Geleijns, H.J. Lamb, E.E. van der Wall, A. de Roos, M.J. Schalij, Atrial fibrillation: multi-detector row CT of pulmonary vein anatomy prior to radiofrequency catheter ablation--initial experience, *Radiology.* 234 (2005) 702–709.
- [18] W. Seeger, Y. Adir, J.A. Barberà, H. Champion, J.G. Coghlan, V. Cottin, T. De Marco, N. Galiè, S. Ghio, S. Gibbs, et al, Pulmonary hypertension in chronic lung diseases, *J. Am. Coll. Cardiol.* 62(25 Suppl) (2013) D109–116.
- [19] J.M. Wells, G.R. Washko, M.K. Han, N. Abbas, H. Nath, A.J. Marmar, E. Regan, W.C. Bailey, F.J. Martinez, E. Westfall, et al, Pulmonary arterial enlargement and acute exacerbations of COPD, *N. Engl. J. Med.* 367 (2012) 913–921.
- [20] S. Matsuoka, G.R. Washko, M.T. Dransfield, T. Yamashiro, R. San Jose Estepar, A. Diaz, E.K. Silverman, S. Patz, H. Hatabu, Quantitative CT measurement of cross-sectional area of small pulmonary vessel in COPD: correlations with emphysema and airflow limitation, *Acad. Radiol.* 17 (2010) 93–99.
- [21] P. Cronin, A.M. Kelly, B.H. Gross, B. Desjardins, S. Patel, E.A. Kazerooni, R.C. Carlos, Reliability of MDCT in characterizing pulmonary venous drainage, diameter and distance to first bifurcation: an interobserver study, *Acad. Radiol.* 14 (2007) 437–444.
- [22] D.M. Hansell, A.A. Bankier, H. MacMahon, T.C. McLoud, N.L. Müller, J. Remy, Fleischner Society: glossary of terms for thoracic imaging, *Radiology.* 246 (2008) 697–722.
- [23] F. van den Hoogen, D. Khanna, J. Fransen, S.R. Johnson, M. Baron, A. Tyndall, M. Matucci-Cerinic, R.P. Naden, T.A. Medsger Jr, P.E. Carreira, et al, 2013 classification criteria for systemic sclerosis: an American College of Rheumatology/European League Against Rheumatism Collaborative Initiative, *Ann. Rheum. Dis.* 72 (2013) 1747–1755.

- [24] A.S. Iyer, J.M. Wells, S. Vishin, S.P. Bhatt, K.M. Wille, M.T. Dransfield, CT scan-measured pulmonary artery to aorta ratio and echocardiography for detecting pulmonary hypertension in severe COPD, *Chest*. 145 (2014) 824–832.
- [25] L. Todorovich-Hunter, D.J. Johnson, P. Ranger, F.W. Keeley, M. Rabinovitch, Altered elastin and collagen synthesis associated with progressive pulmonary hypertension induced by monocrotaline. A biochemical and ultrastructural study, *Lab. Invest.* 58 (1988) 184–191.
- [26] W.W. Wagner, P. Hervé, Physiology of pulmonary capillary recruitment, *Rev. Mal Respir.* 6 (1989) 39–44.
- [27] J.N. Pande, J.M. Hughes, Regional pulmonary clearance of inhaled $C^{15}O$ and $C^{15}O_2$ in man at rest and during exercise. *Clin. Physiol.* 3 (1983) 491–501.
- [28] A. Morales-Cárdenas, C. Pérez-Madrid, L. Arias, P. Ojeda P, M.P. Mahecha, A. Rojas-Villarraga, J.A. Carrillo-Bayona, J.M. Anaya, Pulmonary involvement in systemic sclerosis, *Autoimmun. Rev.* 15 (2016) 1094–1108.
- [29] R. Naeije, N. Chesler, Pulmonary circulation at exercise, *Compr. Physiol.* 2 (2012) 711–741.
- [30] S.A. van Wolferen, J.T. Marcus, A. Boonstra, K.M. Marques, J.G. Bronzwaer, D.M. Spreeuwenberg, P.E. Postmus, A. Vonk-Noordegraaf, Prognostic value of right ventricular mass, volume, and function in idiopathic pulmonary arterial hypertension, *Eur. Heart. J.* 28 (2007) 1250–1257.
- [31] M.C. van de Veerdonk, T. Kind, J.T. Marcus, G.J. Mauritz, M.W. Heymans, H.J. Bogaard A. Boonstra, K.M. Marques, N. Westerhof, A. Vonk-Noordegraaf. Progressive right ventricular dysfunction in patients with pulmonary arterial hypertension responding to therapy, *J. Am. Coll. Cardiol.* 58 (2011) 2511–2519.
- [32] S.C. Mathai, S.K. Danoff, Management of interstitial lung disease associated with connective tissue disease, *BMJ.* 352 (2016) h6819.
- [33] A. Boueiz, S.C. Mathai, L.K. Hummers, P.M. Hassoun, Cardiac complications of systemic sclerosis: recent progress in diagnosis, *Curr. Opin. Rheumatol.* 22 (2010) 696–703.
- [34] V.O. Chan, S. McDermott, O. Buckley, S. Allen, M. Casey, R. O'Laoide, W.C. Torreggiani, The relationship of body mass index and abdominal fat on the radiation dose received during routine computed tomographic imaging of the abdomen and pelvis, *Can. Assoc. Radiol. J.* 63 (2012) 260–266.
- [35] L.G. Rudski, W.W. Lai, J. Afilalo, L. Hua, M.D. Handschumacher, K. Chandrasekaran, S.D. Solomon, E.K. Louie, N.B. Schiller, Guidelines for the echocardiographic assessment of the right heart in adults: a report from the American Society of Echocardiography endorsed by the European Association of Echocardiography, a registered branch of the European Society of Cardiology, and the Canadian Society of Echocardiography, *J. Am. Soc. Echocardiogr.* 23

(2010) 685–713.

FIGURE LEGENDS

Fig 1. Measurement of PA, Ao, and PVD.

(A) The interpreter measured the diameter of the main pulmonary artery at the level of its bifurcation (pulmonary artery) and the diameter of the ascending aorta in its maximum dimension (Ao) using the same images.

(B) We chose a short-axis computed tomography image that showed the ostium of the right inferior pulmonary vein at its widest diameter, and then measured the PVD.

Abbreviations: Ao, aorta; PA, pulmonary artery; PA/Ao, ratio of the diameter of the pulmonary artery to that of the aorta; PVD, ostial diameter of the right inferior pulmonary vein

Fig 2. Selection of patients with PAH.

We measured the diameters of the PA, Ao, and PVD and calculated the PA/Ao in 45 subjects (PAH group). PVD was not measurable in one patient because of distortion caused by parenchymal fibrosis. %CSA_{<5} was calculated in only 20 of these 45 subjects (%CSA_{<5} group), because of use of contrast medium or inadequate CT acquisition parameters in the remaining 25 subjects.

Abbreviations: %CSA_{<5}, cross-sectional area of small pulmonary vessels <5 mm² as a percentage of total lung area; CT, computed tomography; FEV₁, forced expiratory volume in 1 second; FVC, forced vital capacity; PA/Ao, ratio of the diameter of the pulmonary artery to that of the aorta; PAH, pulmonary arterial hypertension; PVD, ostial diameter of the right inferior pulmonary vein

Fig 3. PA/Ao, %CSA_{<5}, and PVD in patients with PAH and in controls.

Both PA/Ao and %CSA_{<5} are significantly higher in the patients with PAH than in the controls,

but there is no significant difference in PVD between the two groups.

Abbreviations: %CSA_{<5}, cross-sectional area of small pulmonary vessels <5 mm² as a percentage of total lung area; NS, not statistically significant; PA/Ao, ratio of the diameter of the pulmonary artery to that of the aorta; PAH, pulmonary arterial hypertension; PVD, ostial diameter of the right inferior pulmonary vein

Fig 4. Results of ROC analyses of PA/Ao, %CSA_{<5}, and PVD for the diagnosis of pulmonary arterial hypertension.

ROC analyses for diagnosis of pulmonary arterial hypertension showed a high AUC for PA/Ao (0.955) and modest AUCs for %CSA_{<5} (0.748) and for PVD (0.560).

Abbreviations: %CSA_{<5}, cross-sectional area of small pulmonary vessels <5 mm² as a percentage of total lung area; Ao, aorta; AUC, area under the curve; PA, pulmonary artery; PA/Ao, ratio of the diameter of the pulmonary artery to that of the aorta; PVD, ostial diameter of the right inferior pulmonary vein

Fig 5. Relationships between right heart catheterization parameters and the PA/Ao, %CSA_{<5}, and PVD.

(A) PA/Ao correlates positively with mPAP but not with CI and PVR.

(B) PVD correlates negatively only with PVR. (C) %CSA_{<5} correlates negatively with mPAP and PVR and positively with CI.

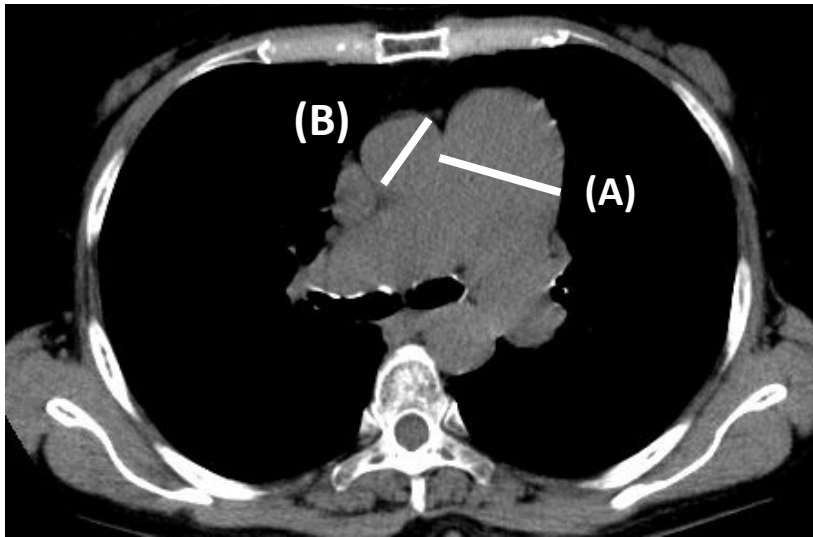
Abbreviations: %CSA_{<5}, cross-sectional area of small pulmonary vessels <5 mm² as a percentage of total lung area; Ao, aorta; CI, cardiac index; mPAP, mean pulmonary artery pressure; PA, pulmonary artery; PA/Ao, ratio of the diameter of the pulmonary artery to that of the aorta; PAH, pulmonary arterial hypertension; PVD, ostial diameter of the right inferior pulmonary vein; PVR, pulmonary vascular resistance

Fig 6. Relationships between right heart catheterization parameters and the combined parameters of PA/Ao, %CSA_{<5} of the upper slice and PVD.

PA/Ao/(%CSA_{<5} of the upper slice) and PVD/(%CSA_{<5} of the upper slice) show significant correlations with mPAP, PVR, and CI with higher correlation coefficients than PA/Ao, %CSA_{<5} of the upper slice, or PVD alone.

Abbreviations: %CSA_{<5}, cross-sectional area of small pulmonary vessels <5 mm² as a percentage of total lung area; Ao, aorta; CI, cardiac index; mPAP, mean pulmonary artery pressure; PA, pulmonary artery; PA/Ao, ratio of the diameter of the pulmonary artery to that of the aorta; PAH, pulmonary arterial hypertension; PVD, ostial diameter of the right inferior pulmonary vein; PVR, pulmonary vascular resistance

(A) PA/Ao



(B) PVD

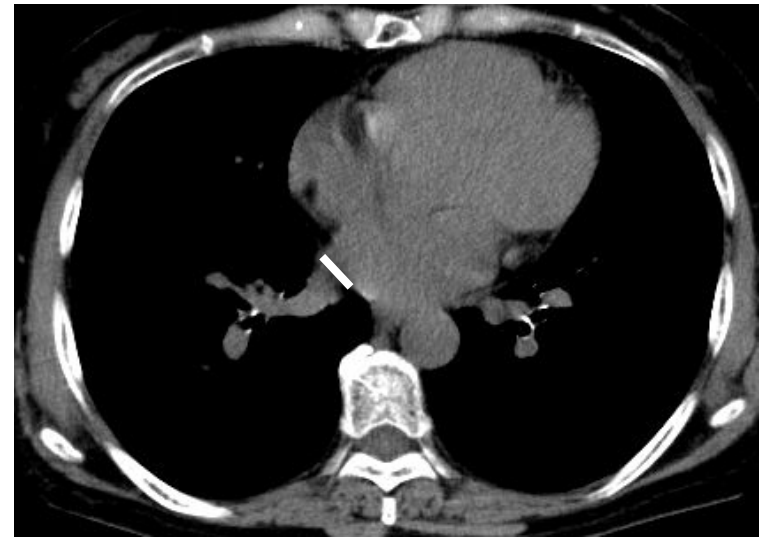


Fig. 1

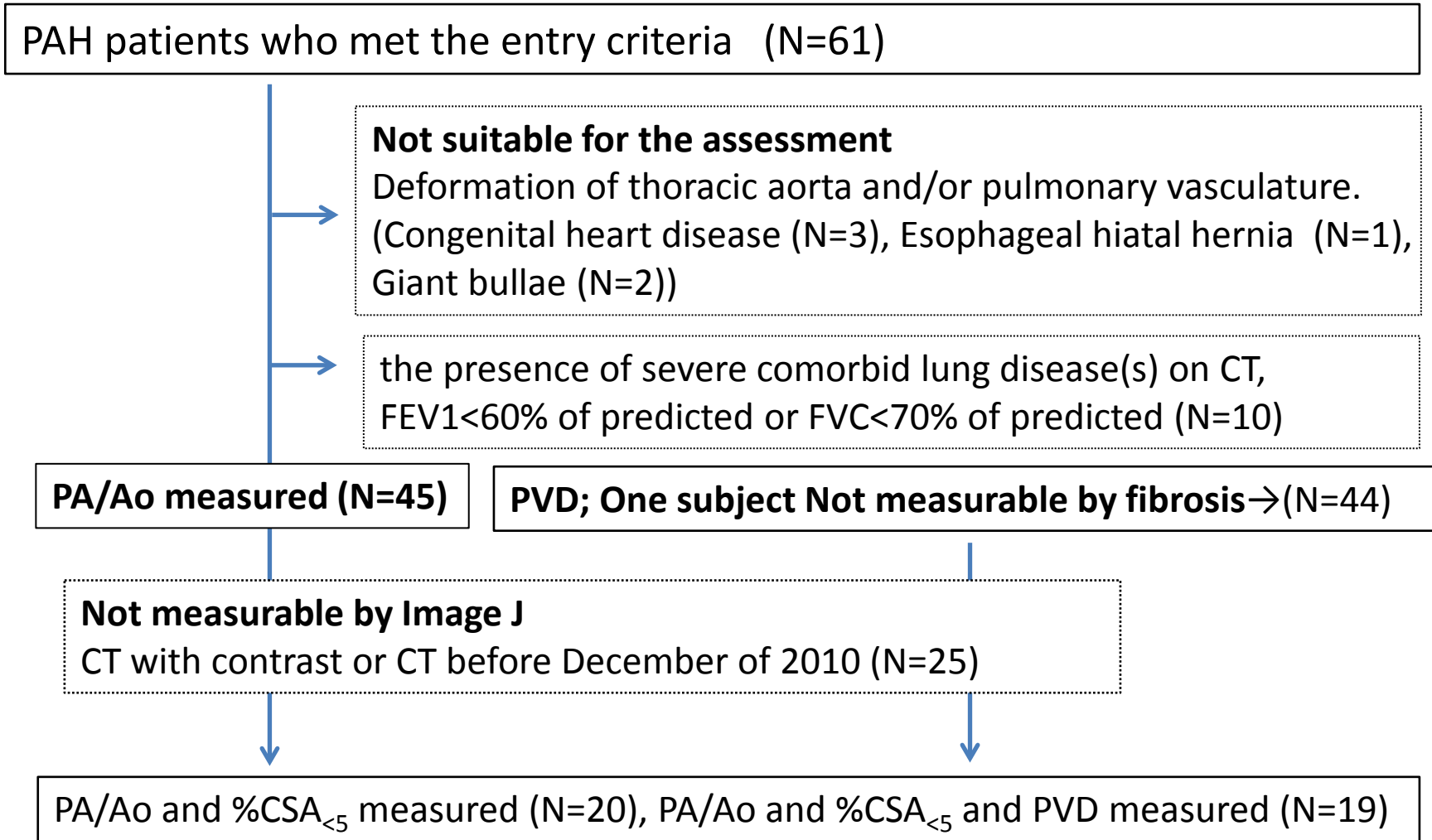
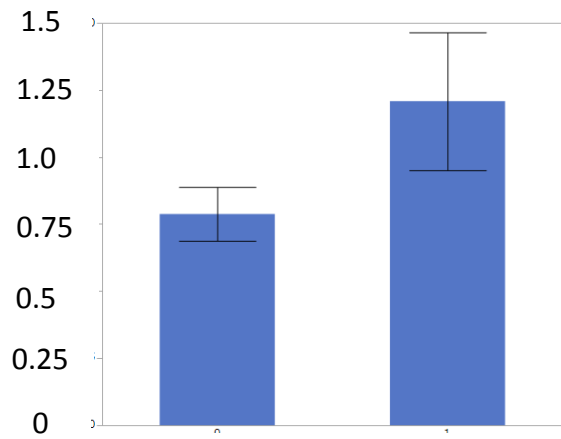


Fig. 2

PA/Ao

P<0.001



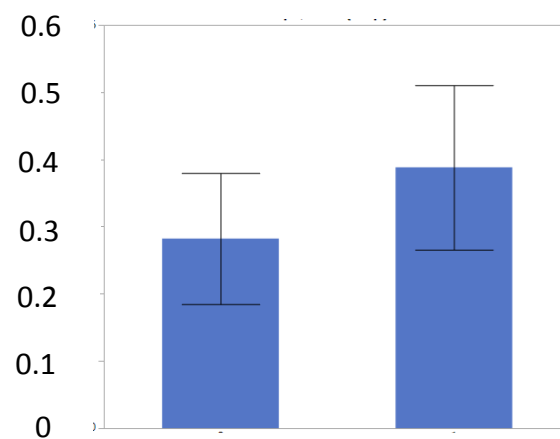
Control
(N=56)

PAH
(N=45)

%CSA_{<5}

P=0.001

[%]



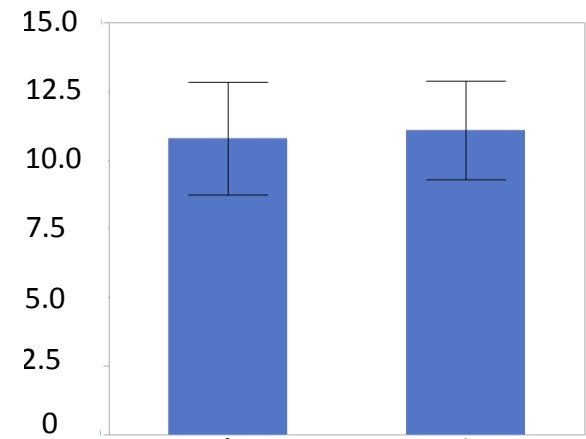
Control
(N=56)

%CSA_{<5}
(N=20)

PVD

N.S.

[mm]

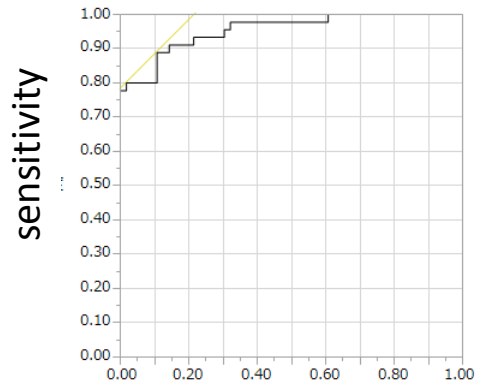


Control
(N=56)

PVD
(N=44)

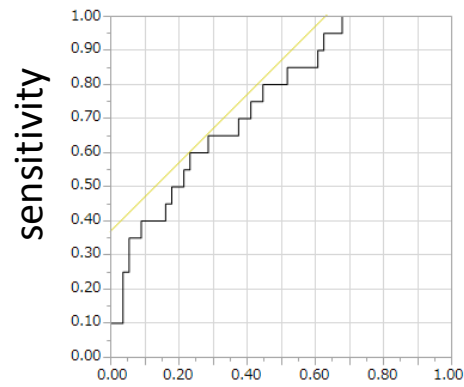
Fig. 3

PA/Ao



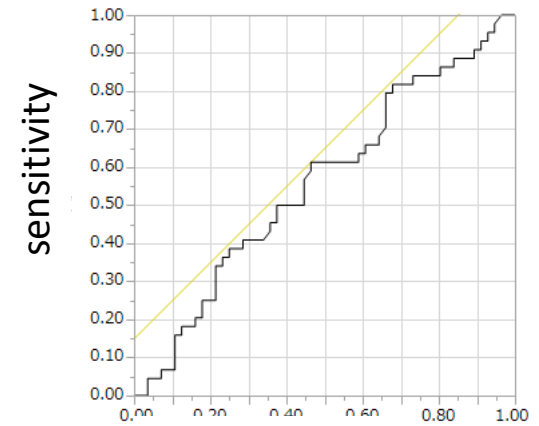
1-specificity
AUC=0.9548

%CSA_{<5}



1-specificity
AUC=0.7482

PVD



1-specificity
AUC=0.5600

Fig. 4

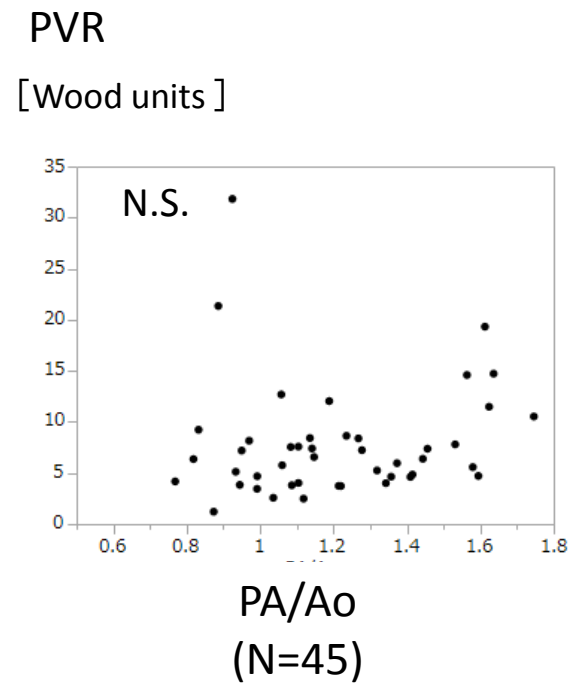
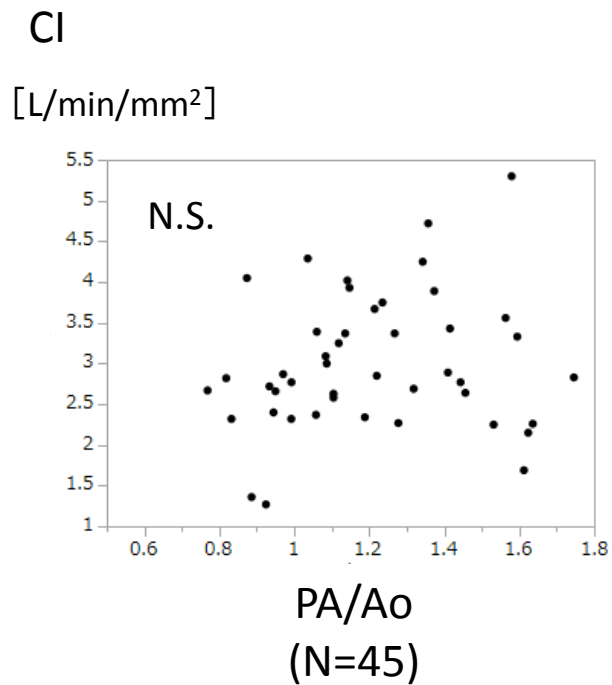
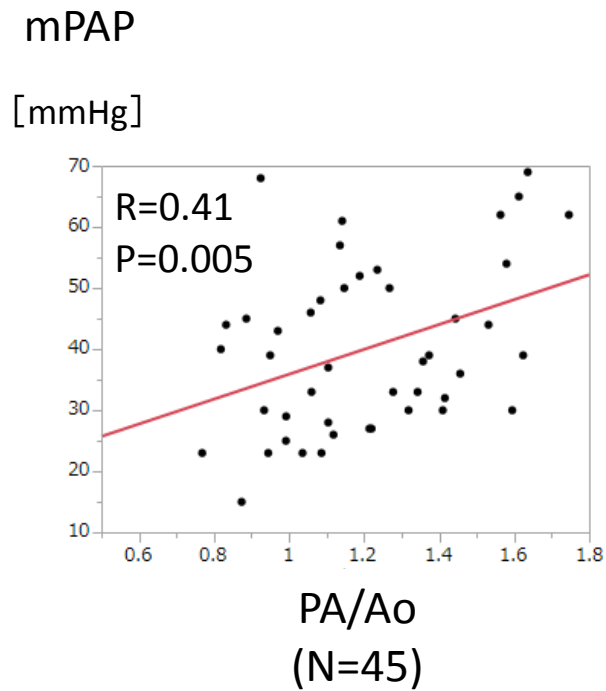


Fig. 5a

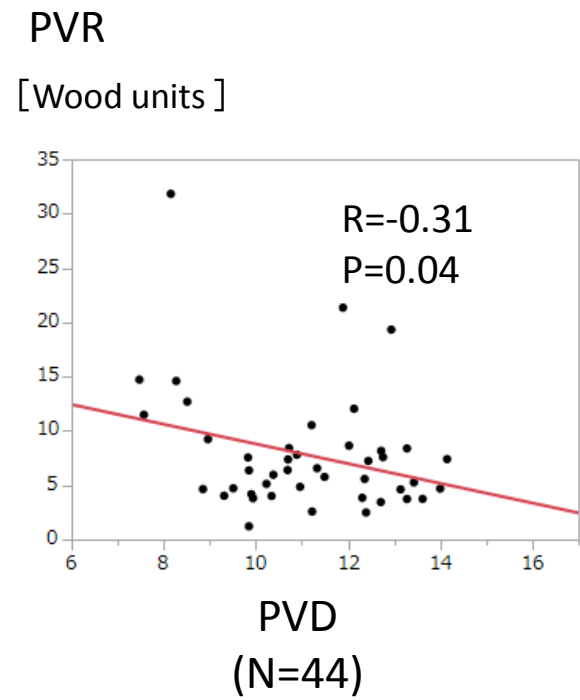
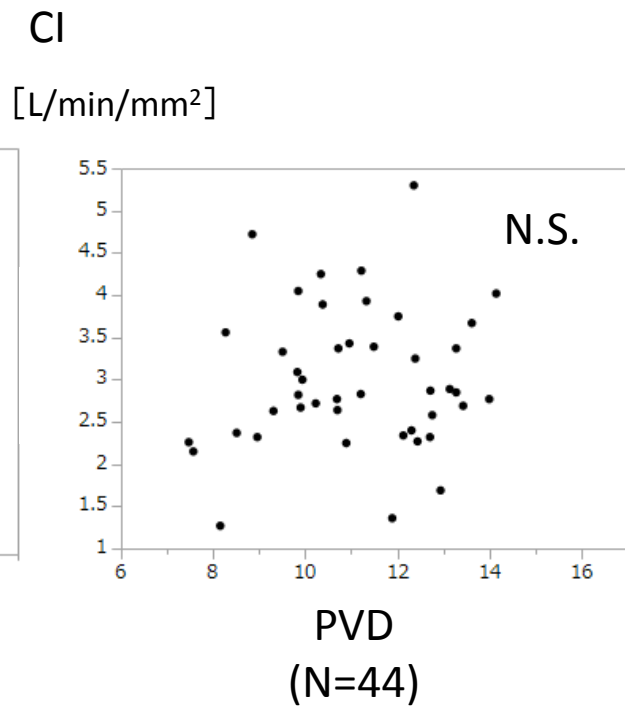
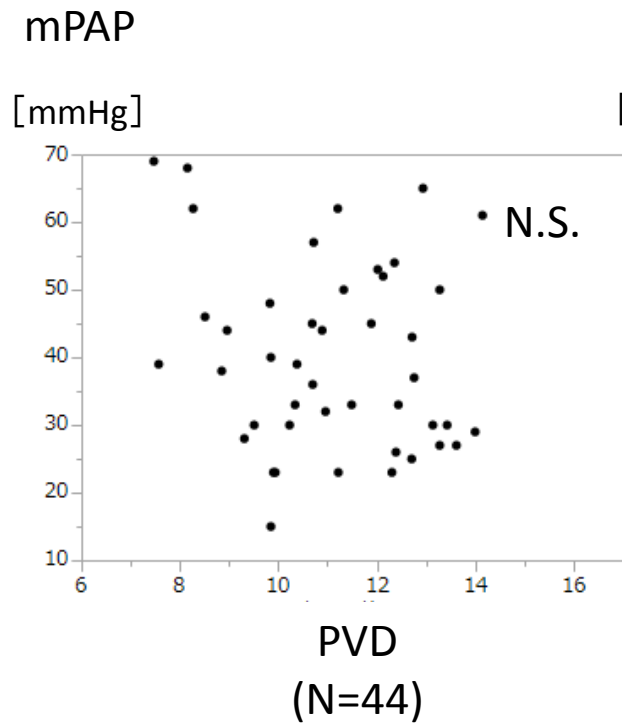
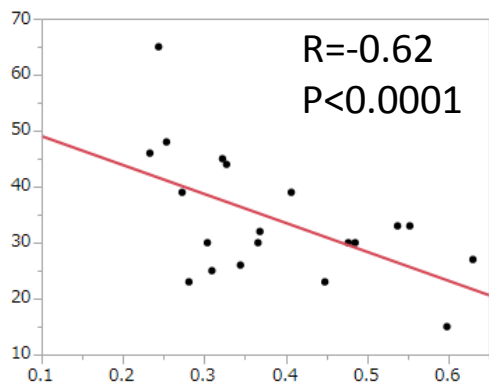


Fig. 5b

mPAP

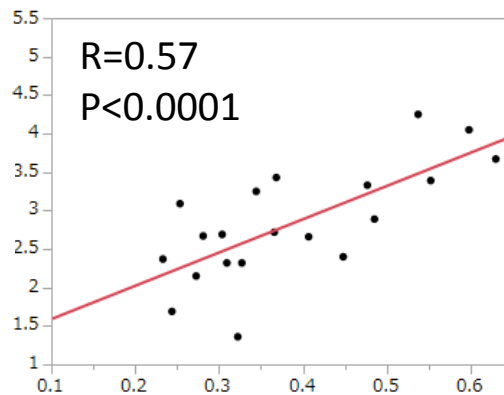
[mmHg]



%CSA<sub>₅
(N=20)</sub>

CI

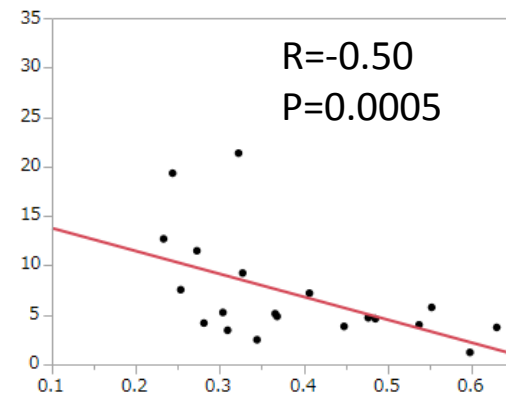
[L/min/mm²]



%CSA<sub>₅
(N=20)</sub>

PVR

[Wood units]

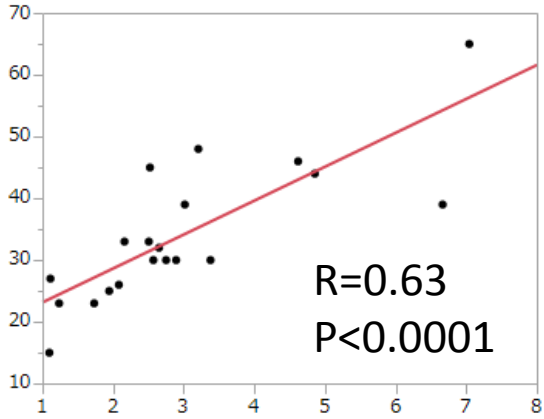


%CSA<sub>₅
(N=20)</sub>

Fig. 5c

mPAP

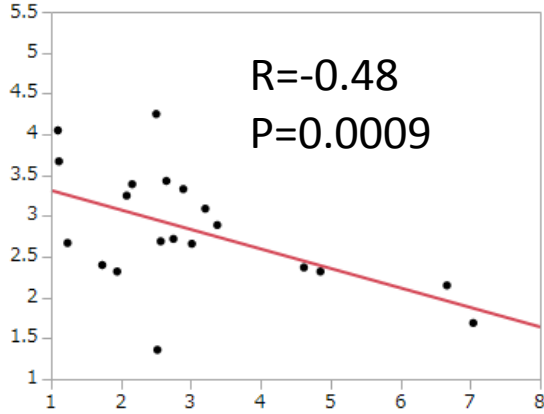
[mmHg]



PA/Ao
/upper %CSA_{<5}
(N=20)

CI

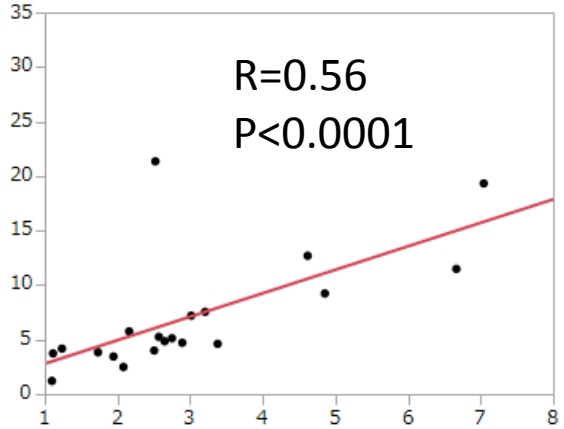
[L/min/mm²]



PA/Ao
/upper %CSA_{<5}
(N=20)

PVR

[Wood units]



PA/Ao
/upper %CSA_{<5}
(N=20)

Fig. 6a

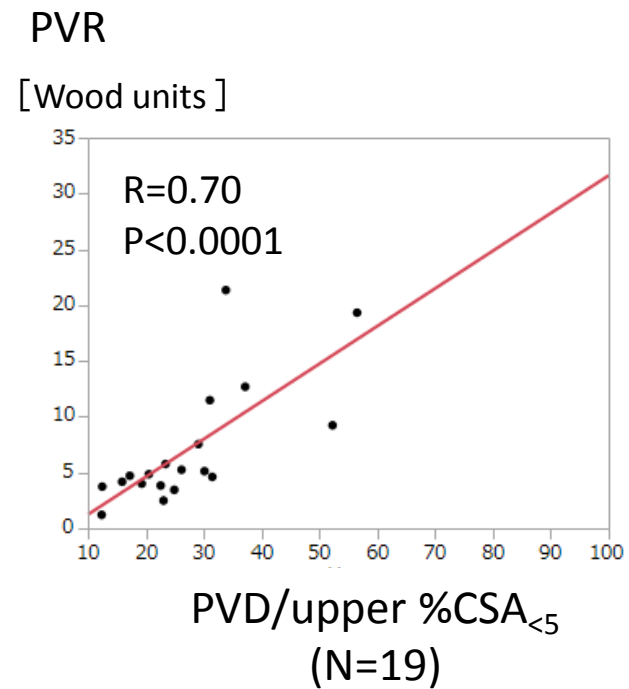
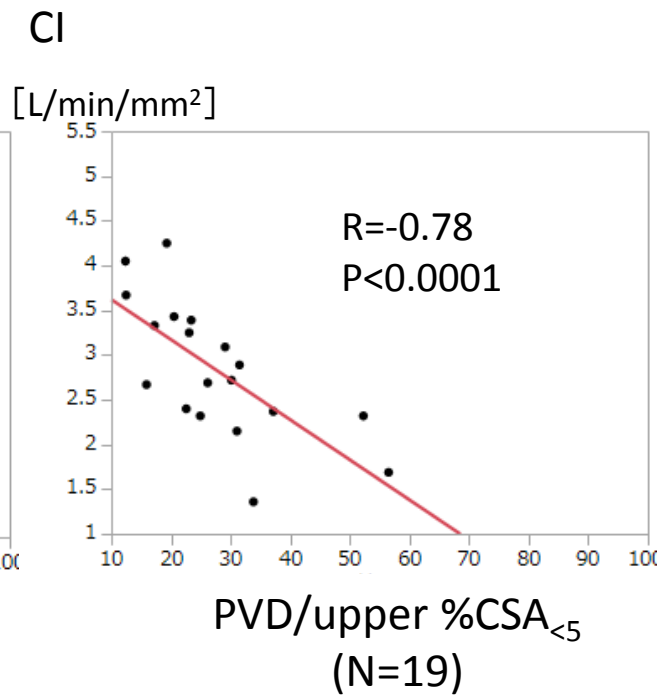
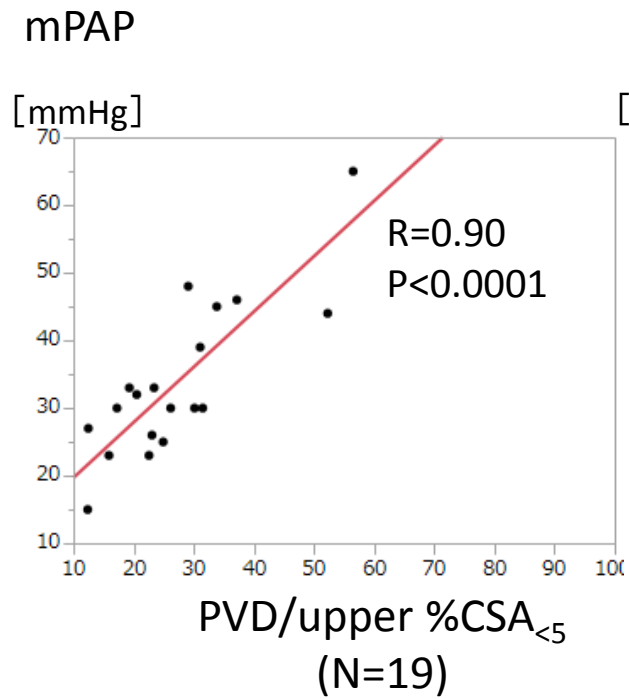


Fig. 6b

Table 1 Demographics of patients with PAH and controls

| Characteristics | PAH | | Control |
|------------------------------------|--------------------|-----------------------------------|--------------------|
| | PA/Ao group | %CSA_{<5} group | |
| Patients, n | 45 | 20 | 56 |
| Age, years | 46.7 ± 14.8 | 49.0 ± 14.9 | 50.5 ± 12.8 |
| Sex, male/female | 3/42 | 1/19 | 1/19 |
| Height, cm | 156.0 ± 7.5 | 155.9 ± 7.9 | 156.9 ± 6.3 (N=48) |
| Weight, kg | 57.0 ± 11.6 | 55.5 ± 11.0 | 56.0 ± 9.8 (N=48) |
| Body mass index, kg/m ² | 23.4 ± 4.3 | 22.7 ± 4.1 | 22.8 ± 4.0 (N=48) |

Data are shown as the mean ± standard deviation. Abbreviations: %CSA_{<5}, cross-sectional area of small pulmonary vessels <5 mm² as a percentage of total lung area; PAH, pulmonary arterial hypertension

Table 2 Pulmonary hypertension-related data for the PA/Ao group and the %CSA_{<5} group

| | PA/Ao group (n = 45) | %CSA_{<5} group (n = 20) |
|---|-----------------------------|--|
| Subgroup of PAH, n (%) | | |
| Idiopathic/heritable | 15 (33%)/3 (7%) | 10 (50%)/0 (0%) |
| Associated with CTD | 22 (49%) | 10 (50%) |
| SSc/non SSc | 6/16 | 4/6 |
| Others | 5 (11%) | 0 (0%) |
| Interstitial lung shadows (Yes/No) | 18/27 | 6/14 |
| BNP, pg/dL | 344.6 ± 1088.0 | 156.1 ± 311.7 |
| Right heart catheterization | | |
| Mean pulmonary artery pressure, mmHg | 40.2 ± 13.7 | 34.4 ± 11.5 |
| Cardiac index, L/min/m ² | 3.0 ± 0.8 | 2.8 ± 0.7 |
| Pulmonary artery wedge pressure, mmHg | 8.4 ± 2.6 | 8.1 ± 2.2 |
| Pulmonary vascular resistance, Wood units | 7.8 ± 5.6 | 7.1 ± 5.3 |
| Use of drug(s) approved for PAH | | |
| No/Yes (single/double/triple) | 21/24 (9/2/13) | 6/14 (5/0/9) |
| PGI2 analogs (intravenous/oral) | 4/17 | 3/9 |
| PDE5 inhibitors (tadalafil/sildenafil) | 6/7 | 6/4 |
| ERAs (ambrisentan/bosentan) | 6/11 | 5/5 |

Data are shown as the mean ± standard deviation. Abbreviations: %CSA_{<5}, cross-sectional area of small pulmonary vessels <5 mm² as a percentage of total lung area; BNP, brain natriuretic peptide; CTD, connective tissue disease; ERAs, endothelin receptor antagonists; PAH, pulmonary arterial hypertension; PDE5, phosphodiesterase type 5; PGI2, prostaglandin I2; SSc, systemic sclerosis

Table 3. %CSA_{<5} in patients with PAH and controls

| | %CSA _{<5} | | p-value |
|------------------|-----------------------|-------------|---------|
| | PAH | Controls | |
| Mean of 3 slices | 0.39 ± 0.12 | 0.28 ± 0.10 | 0.001 |
| Upper slice | 0.47 ± 0.22 | 0.38 ± 0.14 | 0.08 |
| Middle slice | 0.34 ± 0.15 | 0.22 ± 0.11 | <0.001 |
| Lower slice | 0.35 ± 0.14 | 0.25 ± 0.09 | 0.002 |

Data are shown as the mean ± standard deviation. Abbreviations: %CSA_{<5}, cross-sectional area of small pulmonary vessels <5 mm² as a percentage of total lung area; PAH, pulmonary arterial hypertension

Table 4. Sensitivity, specificity, PPV, and NPV of the computed tomography indices for diagnosis of pulmonary hypertension

| | Cut-off | Sensitivity | Specificity | PPV | NPV |
|-----------------------|---------|-------------|-------------|-------|-------|
| PA/Ao | 0.990 | 0.778 | 1.000 | 0.778 | 1.000 |
| | 1.000 | 0.733 | 1.000 | 0.824 | 0.824 |
| %CSA _{<5} | 0.478 | 0.250 | 0.946 | 0.250 | 0.946 |
| PVD | 14.98 | 0.000 | 0.964 | 0.000 | 0.982 |

Abbreviations: %CSA_{<5}, cross-sectional area of small pulmonary vessels <5 mm² as a percentage of total lung area; NPV, negative predictive value; PA/Ao, ratio of the diameter of the pulmonary artery to that of the aorta; PPV, positive predictive value; PVD, ostial diameter of the right inferior pulmonary vein

Table 5. Correlations of %CSA_{<5} for the upper, middle or lower slices with right heart catheterization data

| %CSA _{<5} | Mean PAP | CI | PVR |
|-----------------------|--------------------------|-------------------------|-------------------------|
| Upper slice | r = -0.6364, p < 0.0001 | r = 0.4778, p = 0.0010, | r = -0.5164, p = 0.0003 |
| Middle slice | r = -0.3867, p = 0.0087, | r = 0.4008, p = 0.0070, | r = -0.3024, p = 0.0435 |
| Lower slice | NS | NS | NS |

Abbreviations: %CSA_{<5}, cross-sectional area of small pulmonary vessels <5 mm² as a percentage of total lung area; CI, cardiac index; NS, not statistically significant; PAP, pulmonary arterial pressure; PVR, pulmonary vascular resistance

Table 6. Results of multivariate regression analysis with regard to correlations of PA/Ao, %CSA_{<5}, and PVD with right heart catheterization parameters

| | Mean PAP | | CI | | PVR | |
|-----------------------|----------|--------------|-------|--------------|-------|-------------|
| | t | p | t | p | t | p |
| PA/Ao | 2.49 | 0.017 | 1.08 | 0.29 | 0.26 | 0.80 |
| ILS | 1.03 | 0.31 | 1.07 | 0.29 | -0.40 | 0.69 |
| SSc | 1.25 | 0.22 | 0.76 | 0.45 | 0.71 | 0.48 |
| %CSA _{<5} | -2.71 | 0.02 | 3.94 | 0.001 | -2.64 | 0.02 |
| ILS | 0.29 | 0.78 | -0.44 | 0/56 | 0.27 | 0.79 |
| SSc | 0.83 | 0.42 | -0.59 | 0.67 | 1.09 | 0.29 |
| PVD | -1.4 | 0.17 | 0.69 | 0.49 | -2.2 | 0.03 |
| ILS | 0.35 | 0.73 | 0.95 | 0.35 | -0.77 | 0.45 |
| SSc | 1.92 | 0.06 | 0.80 | 0.43 | 1.09 | 0.28 |

Abbreviations: %CSA_{<5}, cross-sectional area of small pulmonary vessels <5 mm² as a percentage of total lung area; CI, cardiac index; ILS, interstitial lung shadow(s); PA/Ao, ratio of the diameter of the pulmonary artery to that of the aorta; PAP, pulmonary arterial pressure; PVD, ostial diameter of the right inferior pulmonary vein; PVR, pulmonary vascular resistance; SSc, systemic sclerosis

Table 7. Correlations of the ratios of PA/Ao and PVD to %CSA_{<5} of the three slice levels with right heart catheterization data

| | Mean PAP | CI | PVR |
|-----------------------------------|----------------------|------------------------|-----------------------|
| PA/Ao/Upper%CSA _{<5} | r = 0.63, p < 0.0001 | r = -0.48, p = 0.0009, | r = -0.56, p < 0.0001 |
| PA/Ao/Middle%CSA _{<5} | NS | r = -0.29, p = 0.050, | NS |
| PA/Ao/Lower%CSA _{<5} | r = 0.30, p = 0.04 | NS | NS |
| PVD/Upper%CSA _{<5} | r = 0.90, p < 0.0001 | r = -0.78, p < 0.0001, | r = 0.70, p < 0.0001 |
| PVD/Middle%CSA _{<5} | NS | NS | NS |
| PVD/Lower%CSA _{<5} | r = 0.37, p = 0.01 | NS | NS |

Abbreviations: %CSA_{<5}, cross-sectional area of small pulmonary vessels <5 mm² as a percentage of total lung area; CI, cardiac index; NS, not statistically significant; PAP, pulmonary arterial pressure; PVR, pulmonary vascular resistance